

The effect of gas bulk rotation on the morphology of the Ly α line.

Juan Nicolás Garavito-Camargo
Advisor: Jaime E. Forero-Romero

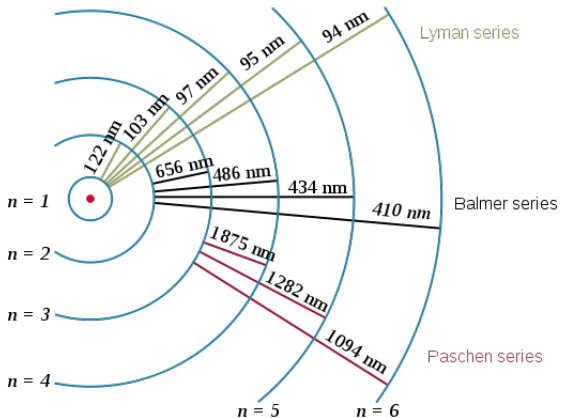
Universidad de los Andes, Bogotá, Colombia

May 20, 2015

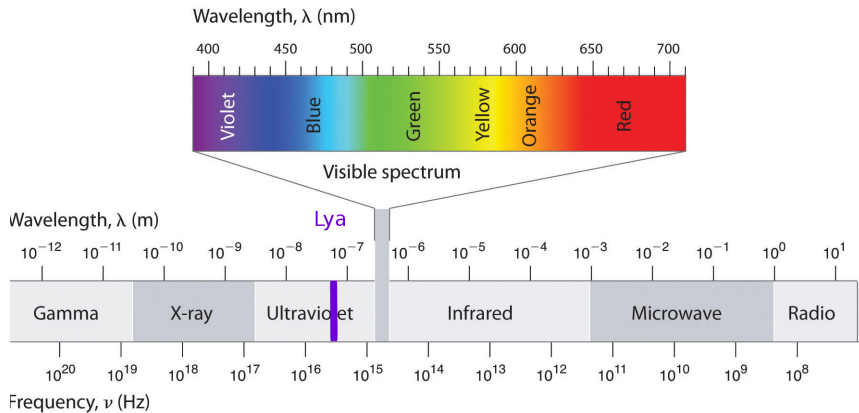


Lyman α emission line:

A Ly α photon is emitted with a $\lambda = 121.56\text{nm}$.



$\text{Ly}\alpha$ is in the vacuum UV part of the EM spectrum



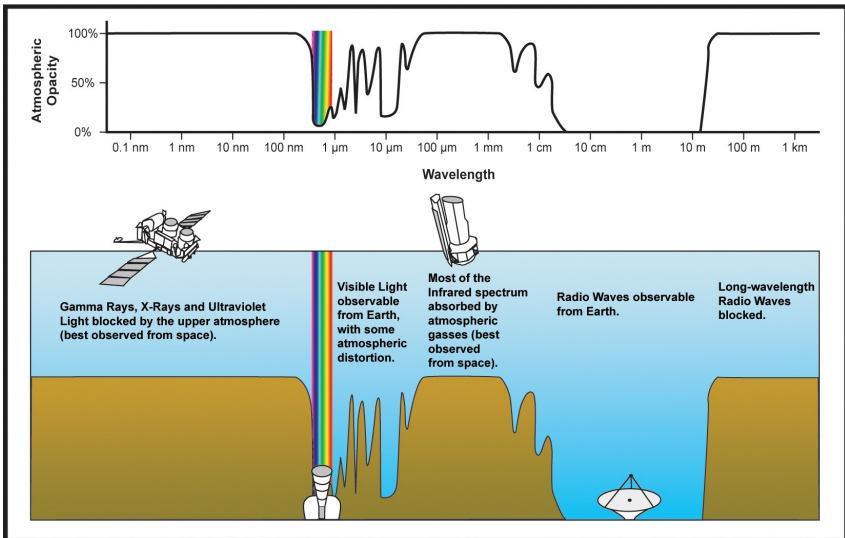


Figure: *

Atmospheric radiation absorption

Cosmological Redshift & the observable LAEs in the visible regime.

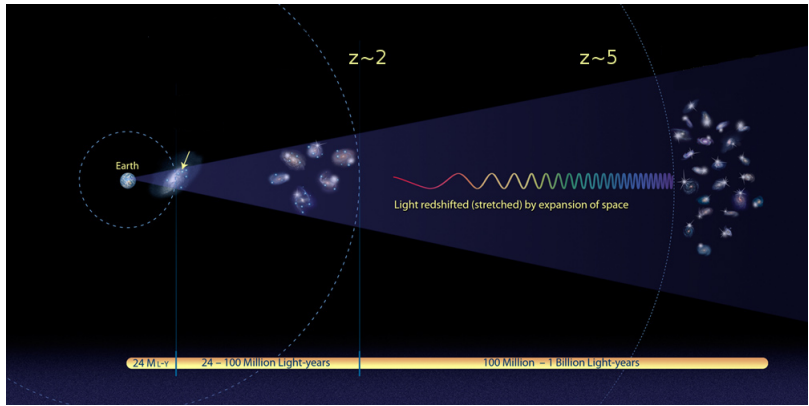


Figure: *

Image credit: NASA, ESA, and A. Feild (STScI).

Do galaxies radiate Ly α photons?

Hydrogen is the most abundant element in the Universe.

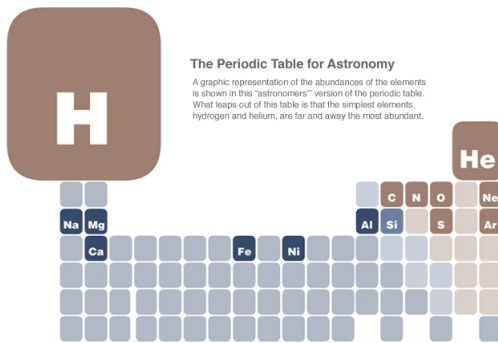


Figure: Astronomers periodic table. Image credit:
<http://chandra.harvard.edu>

UV radiation mechanisms and sources:

- 1.** UV stellar radiation.
- 2.** Gravitational cooling.
- 3.** UV background radiation.

ARE YOUNG GALAXIES VISIBLE?

R. B. PARTRIDGE AND P. J. E. PEEBLES
Palmer Physical Laboratory, Princeton University
Received August 5, 1966; revised September 8, 1966

ABSTRACT

The purpose of this paper is to assess the general possibility of observing distant, newly formed galaxies. To this end a simple model of galaxy formation is introduced. According to the model galaxies should go through a phase of high luminosity in early stages of their evolution. The estimated luminosity for a galaxy resembling our own is $\sim 3 \times 10^{16}$ ergs/sec, roughly 700 times higher than the present luminosity. The bright phase would occur at an epoch of about 1.5×10^8 years, corresponding to a redshift between 10 and 30, depending on the cosmological model assumed.

The possibility of detecting individual young galaxies against the background of the night sky is discussed. Although the young galaxies would be numerous and would have sufficiently large angular diameters to be easily resolved, most of the radiation from the young galaxies would arrive at wavelengths of $1-3 \mu$ where detection is difficult. However, it seems possible that the Lyman- α line might be detected if it is a strong feature of the spectra of young galaxies.

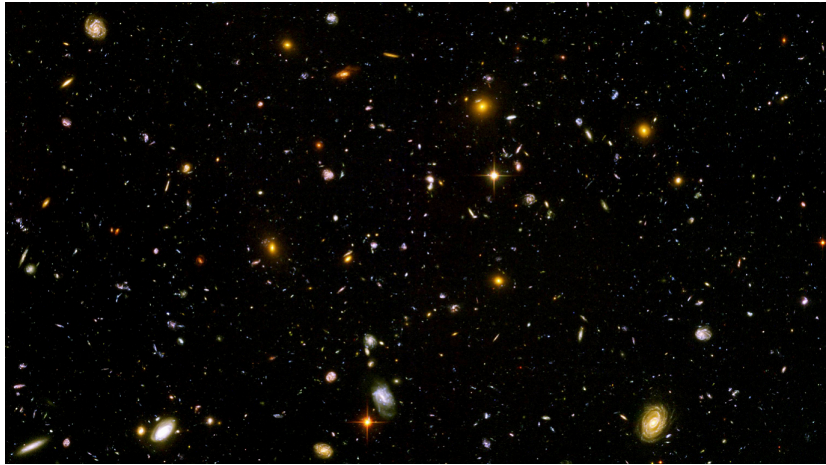
It is also shown how such an experiment might help us to distinguish between various cosmological models.

25 years later ...

SEARCHES FOR PRIMEVAL GALAXIES

S. Djorgovski and D. J. Thompson
Palomar Observatory
California Institute of Technology
Pasadena, CA 91125, USA

ABSTRACT. We review primeval galaxy searches based on the Ly α line emission. Simple arguments are given which suggest that primeval galaxies (interpreted here as ellipticals and bulges undergoing their first major bursts of star formation) should be detectable with present-day technology. Many active objects are now known at large redshifts, which may be plausibly interpreted as young galaxies, but there is so far no convincing detection of a field population of forming normal galaxies. This suggests that either primeval galaxies were obscured, and/or are to be found at higher redshifts, $z_{gf} > 5$.



LAEs observed spectra:

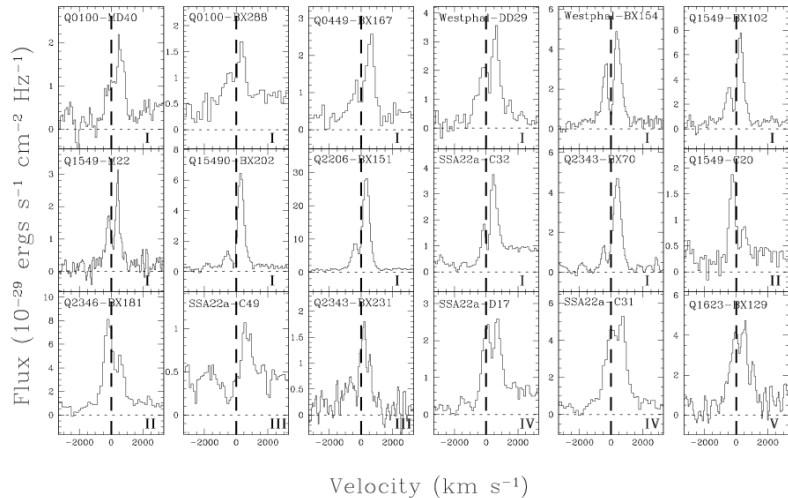
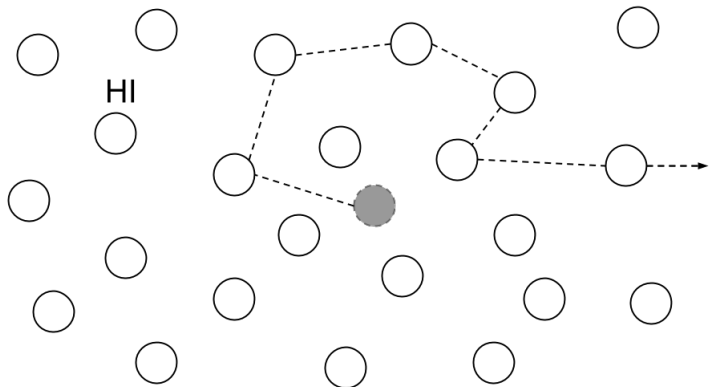


Figure: *

Radiative transfer through a static medium:



Radiative transfer through a non-static medium:

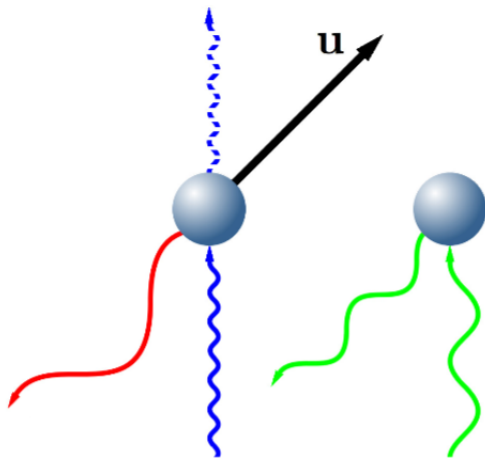
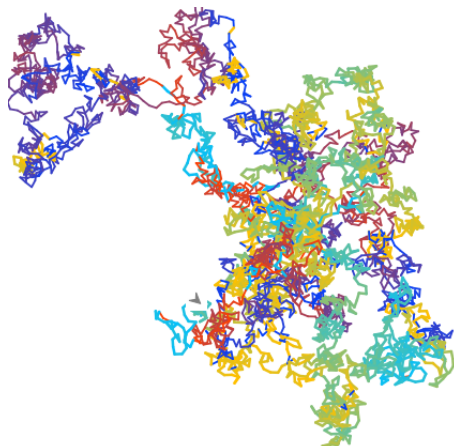


Figure: *

*Ly α photons undergo a random walk in space
and wavelength*



Dust and escape fraction of Ly α photons

Dust grains can either absorb or scatter Ly α photons. The probability of these events is given by the **Albedo (A)**.

$$A = \frac{\sigma_{scatt}}{\sigma_{dust}}$$

The ratio of Ly α photons observed over the Ly α photons emitted define the **escape fraction** f_{esc} .

Radiative transfer theory I:

$$\frac{dJ(\nu)}{d\tau} = \frac{(\Delta\nu_D)^2}{2} \frac{\partial}{\partial\nu} \phi(\nu) \frac{\partial J(\nu)}{\partial\nu} \quad (1)$$

Where ν is the frequency of the photons, $\phi(\nu)$ is the Voigt profile and τ the optical depth.

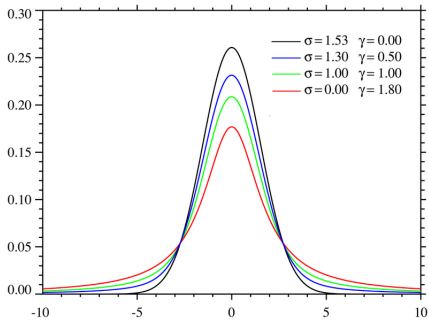


Figure: Voigt profile

Analytical models:

The solution of Eq.?? has been achieved for **two** simplified models: The infinite homogeneous slab and the homogeneous sphere, both with central Ly α sources.

This analytical solution for the slab geometry was derived by Neufeld in 1990.

$$J(\tau, x) = \frac{\sqrt{6}}{24} \frac{x^2}{\sqrt{\pi} a \tau \cosh[\sqrt{\pi^3/54}(x^3 - x_{in}^3)]} \quad (2)$$

Where $a = A/4\pi\Delta\nu_D$ is the voigt parameter and τ the optical depth. Harrington in 1993 derived the frequency at which the line has the maximum intensity:

$$x_m = \pm 1.066(a\tau)^{(1/3)}$$

And the average number of scatterings:

$$N_{scatt} = 1.612\tau$$

Infinite slab spectrum:

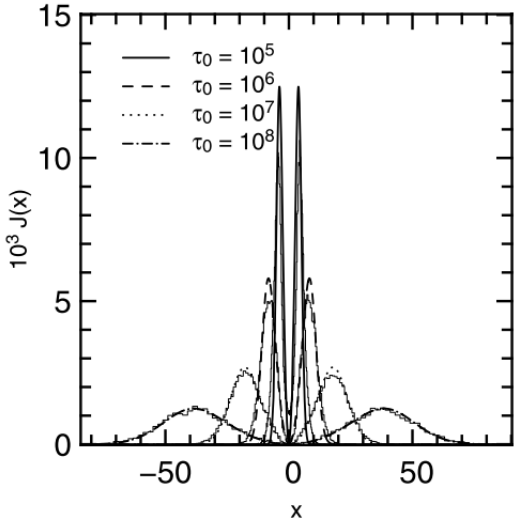


Figure: *

Homogeneous dustless sphere with central sources:

Mark Dijkstra in 2006 has derived the analytical profile of the dustless sphere with central sources.

$$J(\tau, x) = \frac{\sqrt{\pi}}{4\sqrt{6}} \frac{x^2}{a\tau(1 + \cosh[\sqrt{2\pi^3/27}x^3/a\tau])} \quad (3)$$

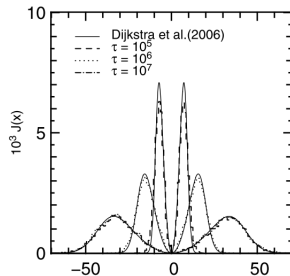


Figure: *

Monte-Carlo approach:

Radiative Transfer via Monte-Carlo methods:

- Set up the initial conditions (Temperature, gas distribution & kinematics).
- Set the Ly α photons initial positions x_{in} .
- Generate the photon random displacement τ_0 in a random direction \vec{n} .
- Derive the HI atom velocity components from the initial field and generate random components for the thermal movements.
- Set the new Ly α direction after the scattering.
- Set the absorption probability due to dust encounters.
- Iterate from step 2.

Expanding/Contracting sphere:

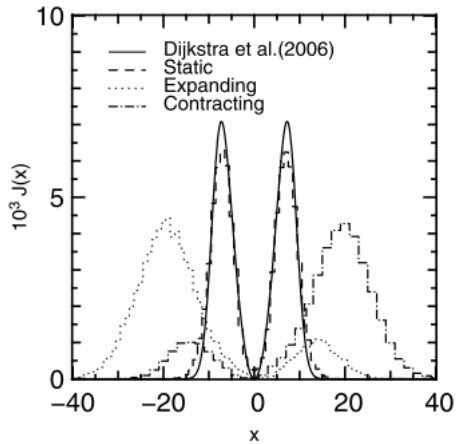


Figure: *

Forero-Romero e.a 2011.

A simulated galaxy spectrum:

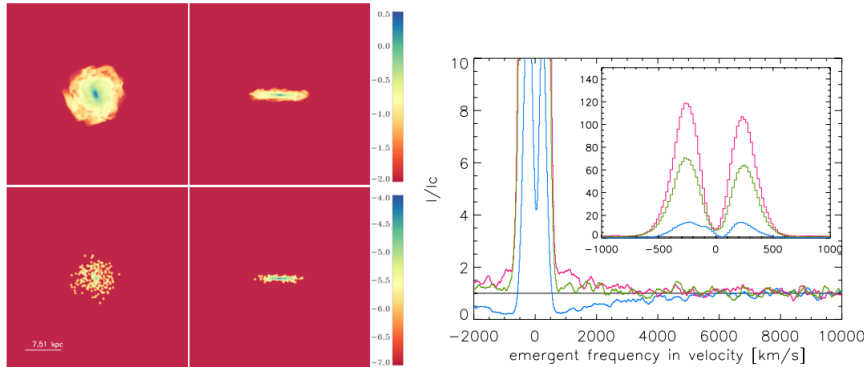
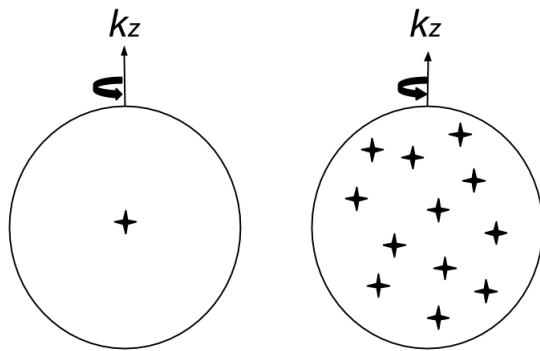


Figure: *

Verhamme, A. e.a, A&A, 2012.

Different geometries and kinematics of the gas have an impact on the morphology of the Ly α spectrum.

What would be the effect of rotation on the morphology of the Ly α line?
Is this effect observable?



Initial conditions:

Initial frequency:

$$x_{in} = \frac{v \cdot k_{in}}{v_{th}}$$

Photon direction:

$$k_{in} = \text{random}$$

Albedo (Probability that the photon is absorbed by the dust grains):

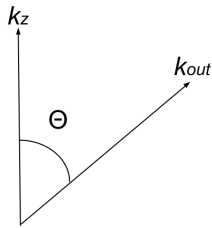
$$A = \frac{1}{2}$$

Models:

Physical Parameter (units)	Symbol	Values
Velocity (km/s)	V_{\max}	0, 100, 200, 300
Hydrogen Optical Depth	τ_H	$10^5, 10^6, 10^7$
Dust Optical Depth	τ_a	0,1
Photons Distributions	Central, Homogeneous	

Table: Summary of Physical Parameters of our Monte Carlo Simulations.

We measure the impact of rotation and viewing angle θ for the main line characteristics.



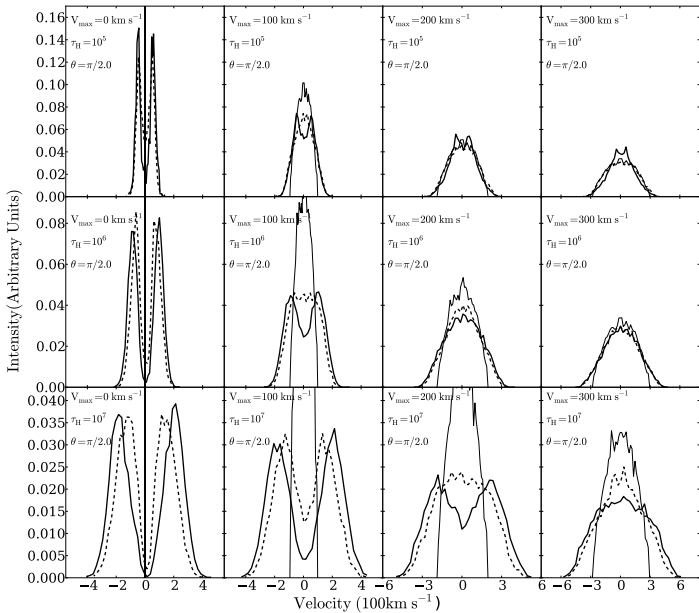


Figure: *

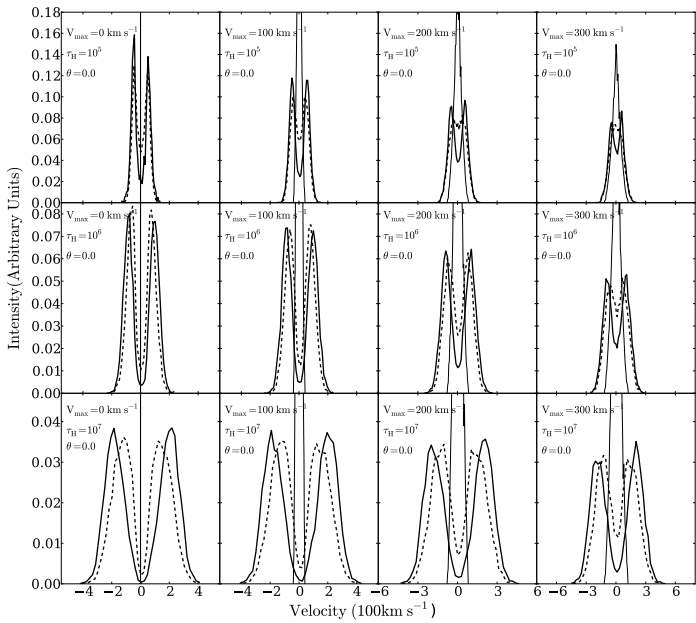


Figure: *

Homogeneous model spectrum:

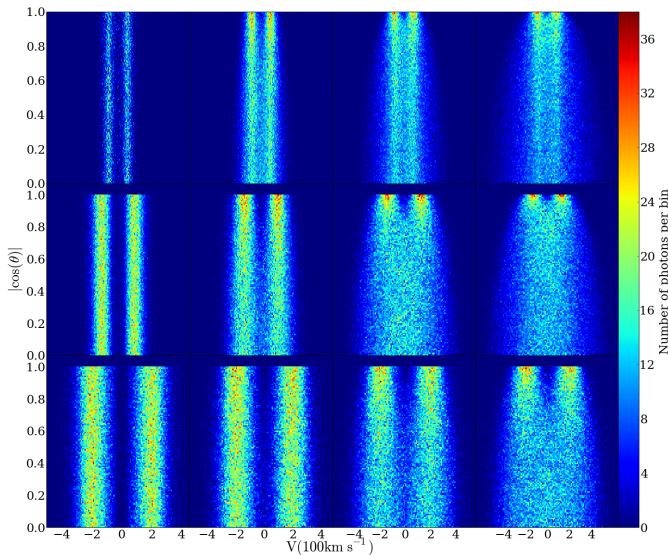


Figure: *

The width of the line increases proportional to the rotation velocity.

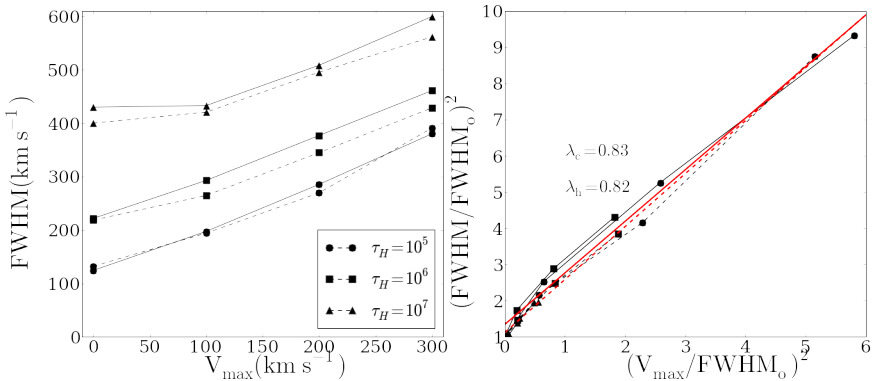


Figure: *

Garavito-Camargo e.a 2014

The width of the line increases proportional to the viewing angle θ

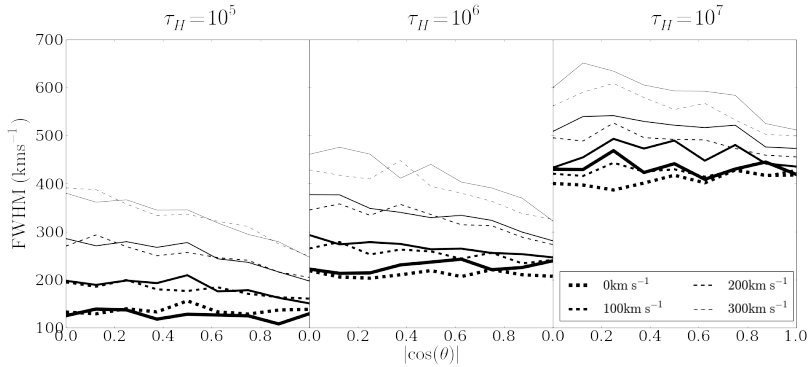


Figure: *

Garavito-Camargo e.a 2014

$$FWHM^2 = FWHM_0^2 + \left(\frac{V_{max}}{\lambda} \right)^2$$

The flux at the line center increases with the rotation velocity and the viewing angle θ .

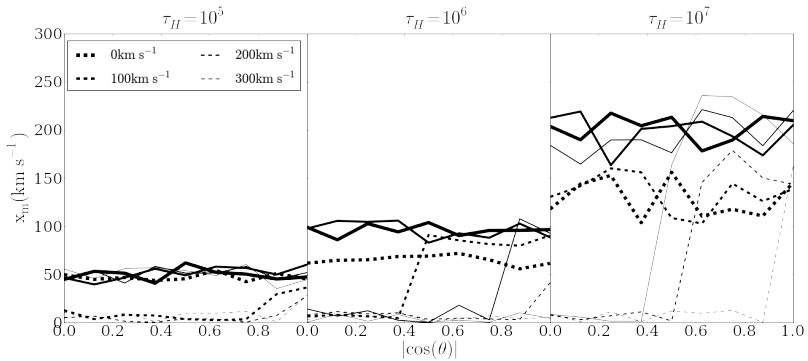


Figure: *

Garavito-Camargo e.a 2014

The average number of scatterings is unaffected by rotation and viewing angle.

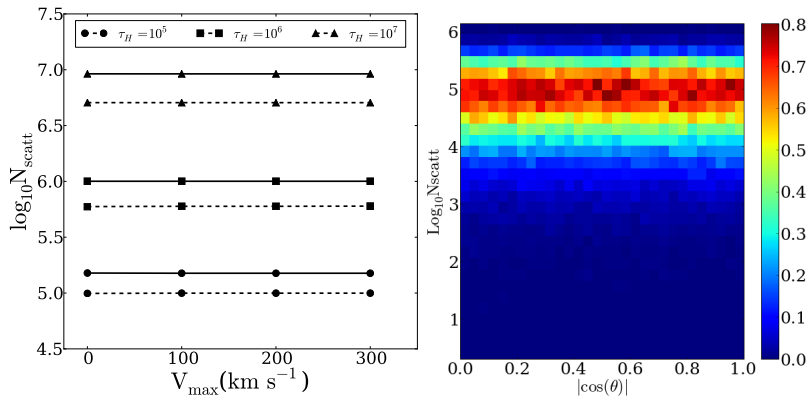


Figure: *

Garavito-Camargo e.a 2014

The escape fraction of Ly α is unaffected by rotation and viewing angle.

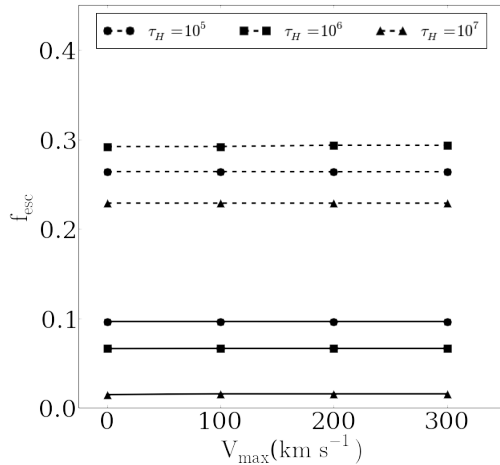


Figure: *

Analytic approximation:

$$J(x, b, \phi, i) = \frac{\sqrt{\pi}}{\sqrt{24}a\tau} \left(\frac{(x - x_b)^2}{1 + \cosh[\sqrt{\frac{2\pi^3}{27}} \frac{|(x - x_b)^3|}{a\tau}]} \right) \quad (4)$$

$$J(x, i) = 2\pi \int_0^R dbb \int_0^{2\pi} d\phi S(b, \phi) J(x, b, \phi, i) \approx 2\pi \int_0^R dbb \int_0^{2\pi} d\phi J(x, b, \phi, i) \quad (5)$$

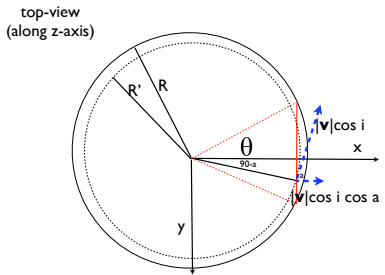
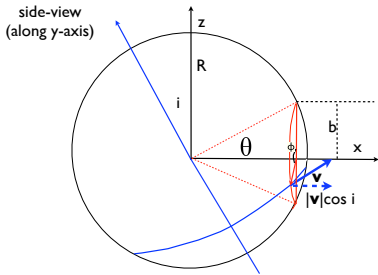


Figure: *

Garavito-Camargo e.a 2014

$$v_b(b, \phi, i) = V_{max} \frac{\sqrt{R^2 - s^2}}{R} \cos i \cos \alpha \quad (6)$$

$$\tan \beta = \tan |90^\circ - \alpha| = \frac{c}{d} = \frac{b \sin \phi}{\sqrt{R^2 - b^2}} \quad (7)$$

Analytic approximation:

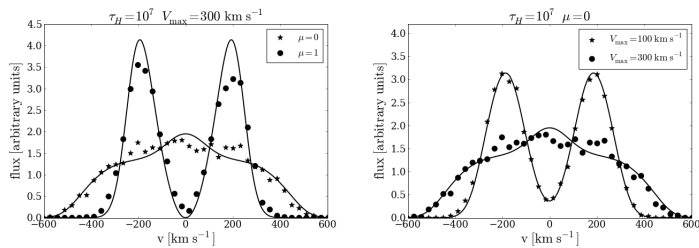
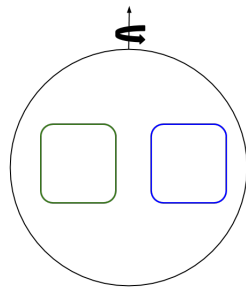


Figure: *

Garavito-Camargo e.a 2014

Lyman alpha observed in rotation:



Conclusions:

1. Rotation has an impact in the Ly α line morphology; the width and the relative intensity of the peaks and the center of the line are affected. For high velocities the line broadens and becomes single peaked. This broadens follows:

$$FWHM^2 = FWHM_0^2 + \left(\frac{V_{max}}{\lambda} \right)^2$$

Conclusions:

2. Rotation induces an anisotropy for different viewing angles, for viewing angles close to the pole the line are double peaked and the line makes a transition to single peaked for viewing angles along the equator.

Conclusions:

- 3.** The escape fraction f_{esc} , the average number of scatterings N_{scatt} and the integrated flux of the line are not affected by rotation neither by the viewing angle.

Work in progress

Fit of the line

Work in progress

rotation + outflows